

Genome-wide studies highlight indirect links between human replication origins and gene regulation

Jean-Charles Cadoret^{†‡}, Françoise Meisch^{†‡}, Vahideh Hassan-Zadeh^{†‡}, Isabelle Luyten[§], Claire Guillet^{¶||}, Laurent Duret^{¶||}, Hadi Quesneville[‡], and Marie-Noëlle Prioleau^{††‡‡}

[†]Institut Jacques Monod, Centre National de la Recherche Scientifique, University Paris 7, 75251 Paris Cedex 5, France; [‡]Université Pierre et Marie Curie, 75005 Paris, France; [§]Unité de Recherches en Génomique-Info, Institut National de la Recherche Agronomique, 91000 Évry, France; [¶]Centre National de la Recherche Scientifique, Université Lyon 1; and ^{||}Unité Mixte de Recherche 5558, Laboratoire de Biométrie et Biologie Evolutive, 69622 Villeurbanne, France

Edited by Gary Felsenfeld, National Institutes of Health, Bethesda, MD, and approved July 14, 2008 (received for review May 28, 2008)

To get insights into the regulation of replication initiation, we systematically mapped replication origins along 1% of the human genome in HeLa cells. We identified 283 origins, 10 times more than previously known. Origin density is strongly correlated with genomic landscapes, with clusters of closely spaced origins in GC-rich regions and no origins in large GC-poor regions. Origin sequences are evolutionarily conserved, and half of them map within or near CpG islands. Most of the origins overlap transcriptional regulatory elements, providing further evidence of a connection with gene regulation. Moreover, we identify c-JUN and c-FOS as important regulators of origin selection. Half of the identified replication initiation sites do not have an open chromatin configuration, showing the absence of a direct link with gene regulation. Replication timing analyses coupled with our origin mapping suggest that a relatively strict origin-timing program regulates the replication of the human genome.

chromatin structure | DNA replication origin | ENCODE regions | genome-wide mapping | CpG island

Controlling the number of origins from which replication begins in a given chromosome is necessary to protect it from instability (1, 2). Mapping DNA replication starting points, known as “origins of replication,” would make a large contribution to understanding how genome replication is coordinated. Identification of a large number of replication origins is necessary to decipher the rules of origin specification. However, fewer than 30 origins have been identified in human cells (3), and they were mapped mostly in well-characterized transcribed regions, leaving gene-poor regions unexplored. The Encyclopedia of DNA Elements (ENCODE) project (4), launched to develop high-throughput methods for identifying functional elements, now provides a comprehensive view of gene expression and chromatin structure along 1% of the human genome (30 Mb, 44 regions) (5); it thus provides a powerful model for studying interactions among chromosome organization, gene regulation, and initiation of DNA replication. Origin selection is initiated by the binding of the origin recognition complex (ORC) to origin-proximal DNA sequences (6). In contrast to *Saccharomyces cerevisiae*, characterized metazoan origins do not conform to a clear consensus sequence, and the ORCs from higher eukaryotes exhibit no sequence specificity *in vitro* (7). Transcription factors at sites of replication initiation have been shown to stimulate replication in many systems, including viruses, yeast, *Drosophila*, and *Xenopus* (8, 9). This stimulation may be a consequence of direct interaction with components of the replication machinery or of facilitating the access of the replication complexes to DNA through recruitment of chromatin remodeling complexes (10–12). Here we present a high-resolution map of replication origins in HeLa cells based on hybridization of short nascent strands (SNS) on DNA microarrays covering ENCODE regions. To construct this map we use one of the most stringent methods for isolating origins of replication based on the resistance of SNS to λ -exonuclease digestion (13). Because only small numbers of short nascent strands can be recovered, they must be amplified before hybridization to the microarray. We chose a method of amplification that gives low

biases, the T7-based DNA linear amplification (TLAD). We thereby mapped 282 origins of replication and confirmed 1 already-known origin, increasing by more than 10-fold the number of currently known origins and constituting a statistically relevant dataset for studying general rules for origin selection.

Results

Identification of 283 Origins Along ENCODE Regions. Because small bubbles of replication are scarce and genome-wide studies based on DNA microarrays require at least 2 μ g of material for hybridization, the development of large-scale studies on the positioning of DNA replication origins is a difficult task. We calculated that if 30,000 origins were activated inside a given cell, we should obtain \approx 10 ng of SNS from 10^8 exponentially growing cells (see *Experimental Procedures*). Two stringent methods have been used successfully to purify sequences located at replication initiation sites. One method relies on the trapping of bubble-shaped structures, and the other is based on isolation of transitory RNA-DNA SNS molecules (13, 14). In the latter method, SNS between 1.5 kb and 2 kb can be purified specifically from an asynchronous population of cells because their RNA primers protect them from λ -exonuclease treatment, whereas broken genomic DNA is digested.

We prepared 5 independent samples of SNS from asynchronous HeLa cells. We coupled the stringent preparation of SNS with the TLAD method, a technique of linear amplification that can generate several μ g of amplified material from 10–20 ng of input DNA (15). We amplified 2 preparations of SNS by TLAD (experiments A and B) for microarray hybridization and cross-checked the results against those obtained by real-time quantitative PCR (qPCR) using the other 3 samples (experiments C, D, and E). The quality of each SNS preparation was tested systematically by qPCR; this test calculated the relative enrichment of an amplicon located near, but not within, the *c-myc* origin (considered as background) relative to an amplicon located inside the *c-myc* origin (defined as 100%). We observed a variation of enrichments that were caused by the accumulation of many critical steps in the SNS purification protocol, namely genomic DNA extraction, polynucleotide kinase treatment, and finally λ -exonuclease digestion. The results were 3%, 15%, 12%, 14%, and 19% for experiments A, B, C, D, and E, respectively. We co-hybridized genomic DNA and SNS amplified by the same technique to reduce possible bias caused by linear amplification. Results obtained on 4 ENCODE regions are shown

Author contributions: J.-C.C., L.D., H.Q., and M.-N.P. designed research; J.-C.C., F.M., V.H.-Z., I.L., C.G., and M.-N.P. performed research; J.-C.C., F.M., V.H.-Z., I.L., C.G., L.D., H.Q., and M.-N.P. analyzed data; and J.-C.C., L.D., H.Q., and M.-N.P. wrote the paper.

The authors declare no conflict of interest.

This article is a PNAS Direct Submission.

Data Deposition: The data reported in this paper have been deposited in the Gene Expression Omnibus (GEO), www.ncbi.nlm.nih.gov/geo (accession no. GSE10217).

^{††}To whom correspondence should be addressed. E-mail: prioleau@ijm.jussieu.fr.

This article contains supporting information online at www.pnas.org/cgi/content/full/0805208105/DCSupplemental.

© 2008 by The National Academy of Sciences of the USA

in supporting information (SI) Figs. S1-S3. To limit the number of false positives, stringent selection criteria were applied for hybridization peak detection (see *Experimental Procedures*). Typical peaks selected from Fig. S1 are presented in Fig. S2. On the 2 DNA microarrays performed, we identified 277 peaks with SNS preparation A and 228 peaks with SNS preparation B; 187 peaks were common to the 2 preparations, and the other 131 peaks were preparation specific. In total, we detected 318 peaks including 187 overlapping peaks. The difference in the quality of SNS preparations A and B (3% versus 15% of background relative to the *c-myc* origin) may explain why origin conservation was only 59% when automatic stringent criteria were applied for peak detection. We then checked each of the 131 preparation-specific peaks individually using slightly less stringent criteria: enriched profile with a similar 1.5-kb width containing among 4 enriched probes at least 2 probes with a p -value $< 10^{-4}$. Ninety-six of these 131 peaks were validated manually on the array where peaks were not automatically detected. Thus, we identified a total of 283 clearly visible peaks on the 2 microarrays (Table S1), corresponding to a final reproducibility of $\approx 90\%$.

Sensitivity and Specificity of Our Genome-Wide Method. To validate the specificity and the sensitivity of our mapping study, we randomly chose 29 of the 283 peaks and 8 background regions and quantified their relative enrichment by qPCR with a third and fourth SNS preparation (experiments C and D) (Fig. S3). All but 1 origin (ori7, 26.5%) had a significant enrichment relative to the *c-myc* background signal (13%; Fig. S3). Amplicons located in the 8 background regions had a very low enrichment, between 2% and 20%. The previously described G6PD origin (16) was found at the same location on our microarrays (Table S1, ori G6PD). For further validation, we analyzed the profile of SNS enrichment of the 5' part of the *HoxA* locus using qPCR with 32 primer pairs and on a fifth preparation confirmed 5 enriched peaks detected by our microarray approach (Fig. S3). These validations demonstrate the specificity and sensitivity of our genome-wide mapping of DNA replication origins. Finally, among 1067 replication origins that have been predicted computationally in the human genome (17), 7 are located within ENCODE regions. Two of these computational predictions fall less than 1 kb from our experimentally identified origins. Although the sample of predicted origins is limited, the overlaps with experimental data are highly significant ($P = 10^{-4}$, Fig. S4).

Primer pairs located in the middle of peaks detected on microarrays were selected for qPCR quantification. The level of enrichment observed by qPCR therefore should indicate origin strength. We observed SNS enrichment ranging from 40% to 330% (Fig. S3), suggesting that our method can detect origins activated in only 12% of cell cycles. This result shows that our microarray approach is sensitive enough to detect weak origins. However, the stringent method applied for peak selection may have missed between 5% and 10% of true positives.

Small ssDNA Are Not Enriched in Short Nascent Strands. A recent paper described a high-throughput mapping of origins of replication in human cells based on a rapid, non-PCR-based hybridization of short ssDNA extracted from asynchronous human cells (18). In this paper, the authors obtained 6–8 μg of 300- to 1000-bp ssDNA from 10^8 cells. This amount is between 2 and 3 orders of magnitude higher than the predicted amount of SNS (see *Experimental Procedures*), suggesting that in this preparation true SNS are swamped by a mass of irrelevant broken genomic DNA. In our study, after λ -exonuclease digestion, we repeatedly obtained ~ 10 ng of 1.5- to 2-kb SNS molecules from 10^8 exponentially growing cells. This amount fits well with the theoretical amount of SNS. In our experiments, before λ -exonuclease treatment, we obtained a much higher yield of single-stranded molecules, $\approx 2 \mu\text{g}$. At this step of purification, we could not detect enrichment of *c-myc* origin by

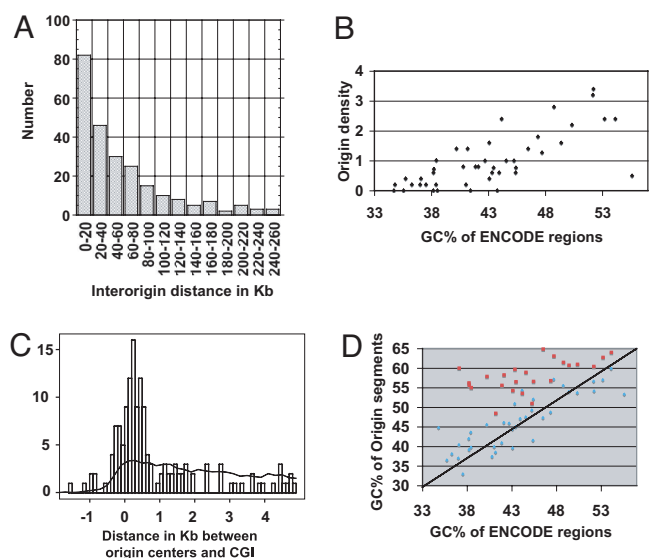


Fig. 1. Strong origins are not evenly distributed along the genome, and a subset of origins is associated with CpG islands. (A) Histogram of the interorigin distances (median = 36080; $n = 245$). Four interorigin distances greater than 260 kb (333, 411, 453, and 480 Kb) are not shown on the graph. (B) Origin density within ENCODE regions correlates with GC richness. The density of origins within each ENCODE region (number of origins per 100 kb) is plotted against the GC percent of the whole region. (C) Origins are enriched in and near CpG islands. The histogram shows the distribution of origin centers relative to CpG islands (CGI). Negative values correspond to origin centers located within CpG islands. The line shows the distribution of the bootstrap sample. (D) Segments containing non-CpG island origins are not enriched in GC. For each ENCODE region, the GC percentage of replication origin segments within CpG islands (red) and outside CpG islands (blue) is plotted against the GC percentage of the whole ENCODE region.

qPCR, showing that, although SNS were in the preparation, the excess of irrelevant broken genomic DNA masks them.

To analyze a preparation of short ssDNA on a larger scale, we co-hybridized on an ENCODE microarray a preparation of 300- to 1000-bp ssDNA with genomic DNA extracted from G_1 cells. We applied for peak detection stringent criteria similar to those used for our SNS study (*Experimental Procedures*). Nine highly significant peaks (Table S2) were identified, and none overlaps with peaks detected with 1.5- to 2-kb SNS. With less stringent criteria (*Experimental Procedures*), we identified 229 peaks (Table S3), including 6 peaks in common with our 283 origin segments. This colocalization is not significant ($P = 0.08$). Moreover, the G6PD origin previously identified is not detected on this microarray. In conclusion, our data show that regions of short ssDNA enrichment do not overlap with peaks obtained with a preparation of SNS stringently purified by λ -exonuclease treatment of 1.5 to 2 kb ssDNA. This result provides a clear demonstration that the identification of replication origins from short ssDNA requires λ -exonuclease digestion.

Origin Density Is Correlated with GC Richness, and Only Half of the Origins Co-Localize with CpG Islands. Whether strong sites of replication initiation are distributed regularly along the human genome remains an open question. The interorigin distances in our sample are diverse (Fig. 1A), ranging from ≈ 1 kb to 500 kb. The mean interorigin distance (~ 63 kb) and most interorigin distances (75% < 81 kb) are within the range of the human replicon size (19). Surprisingly, we found 500-kb regions lacking origins. The base composition of mammalian genomes is very heterogeneous, and gene density is much higher in GC-rich than in GC-poor genomic regions (20, 21). Interestingly, we observe the same pattern for replication origins: replication origin density within ENCODE

containing origins also coincided with H3K4me3 sites. Surprisingly, 46% of the CpG islands lacking origins also overlap with H3K4me3 sites. Thus, we did not detect any significant enrichment of H3K4me3 sites in CpG islands linked to replication origins, relative to all CpG islands. This finding suggests that CpG islands associated with highly transcribed genes are not a better substrate for replication initiation than others. We also tested whether origins outside CpG islands are biased toward an association with H3K4me3 sites. Thirty-two of 184 non-CpG island origins coincided with H3K4me3 sites (17%). Again, we did not detect any H3K4me3 enrichment in this group of origins, relative to the bootstrap sample (14%, $P = 0.025$). From this analysis, we conclude that the link between open chromatin structure and replication initiation sites was only a consequence of the strong association between CpG islands and replication origins. This evidence indicates that although sites of replication initiation are strongly associated with transcription regulatory elements, their use is not favored or impeded by active transcription.

Replication Origins Are Associated Mostly with Regulatory Elements. HS sites identify regions of open chromatin, which encompass all different types of regulatory elements, including promoters, enhancers, silencers, insulators, and locus control regions. DNase-chip analysis on the same ENCODE regions has been performed using 7 human cell lines including HeLa cells (26). We tested whether most of the origins found in HeLa cells mapped within HS sites identified in at least 1 of the cell lines explored. Twenty percent of origins overlap with HS sites found in both HeLa and at least 1 other cell line, whereas only 2% co-localize with HeLa-specific HS sites (Fig. 2C). As additional cell lines are included, the total percentage of origins covered by HS sites increases gradually, reaching 69% at the seventh cell line. We did not detect any significant leveling off after the addition of the seventh cell type. A similar gradual increase in the total percentage of base pairs of the ENCODE regions covered by HS sites has been described previously (26). These findings suggest that HS sites found in additional cell lines may cover almost all the origins identified in our study. The number of HS sites found in the various cell lines that intersect with bootstrap segments increased much more slowly, indicating the significance of this link (red line in Fig. 2C). This analysis provides further evidence for a connection between transcriptional regulatory elements and replication origins.

Replication Origins Are Enriched in Binding Sites of the Transcription Factors c-JUN and c-FOS. The binding of several transcription factors was studied along ENCODE regions in HeLa cells by chromatin immunoprecipitation on chip (ChIP-on-chip), allowing us to test for their role in origin selection. We focused our attention on the AP-1 complex, a dimeric transcription factor comprising c-JUN and c-FOS and known to be a strong driver of the cell cycle from G1 to S phase. We observed a highly significant correlation between origins and c-JUN and c-FOS binding sites ($P < 2.2 \times 10^{-16}$) (Fig. 2D). Fifty-five origins are associated with c-JUN, 53 with c-FOS, and 39 with both. Forty c-JUN origins overlap a CpG island (Fig. 2E). We therefore tested whether the observed link between origins and AP-1 binding sites was the result only of the strong association of origins with CpG islands, as previously shown for H3K4me3. ENCODE regions contain 200 c-JUN binding sites, and 55 of them (27.5%) overlap with replication origins (Fig. 2E). We found that 40% of the CpG islands containing origins also coincided with c-JUN binding sites. However, only 13% of the CpG islands lacking origins also overlap with c-JUN binding sites. Thus, in contrast with H3K4me3, we detected a significant enrichment of c-JUN binding sites in CpG islands linked to replication origins, relative to the rest of CpG islands ($P = 2.2 \times 10^{-16}$). This finding suggests that CpG islands associated with the AP-1 complex are a better substrate for replication initiation than others. We also tested whether origins outside CpG islands are biased toward an association with c-JUN binding sites. Fifteen of 184 non-CpG island origins coincided with

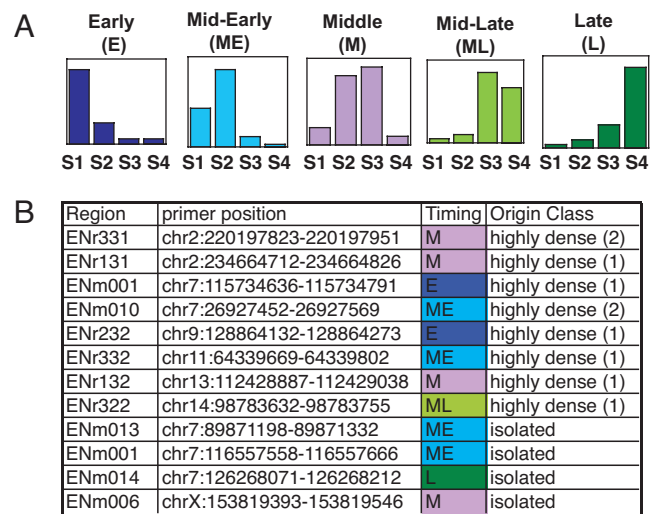


Fig. 3. Isolated origins and clusters of closely spaced origins are activated at all stages in S phase. (A) Replication timing profiles obtained after BrdU pulse labeling, cell sorting, and quantitative PCR were classified into 5 groups according to the enrichment found in fractions S1 to S4. Typical early (E), mid-early (ME), middle (M), mid-late (ML), and late (L) profiles are shown. (B) Timing analysis of highly dense and isolated origins. ENCODE regions, primer pair coordinates used for qPCR, replication timing, and origin class are indicated

c-JUN binding sites (8.1%). Again, we detected c-JUN binding site enrichment in this group of origins relative to the bootstrap sample (3.4%, $P = 3.5 \times 10^{-4}$). We analyzed the intersection of the 55 c-JUN origins with HS and H3K4me3 sites. We again found that a large fraction (40%) had neither an HS site nor H3K4me3 modification, as observed previously in the total group of replication origins (Fig. 2F). From this analysis, we conclude that the link between c-JUN and replication initiation sites is highly significant and is independent of the strong association between replication origins and CpG islands. This result indicates that the AP-1 complex might be an important regulator of replication initiation along the human genome.

A Precise Timing Program Regulates the Timing of Origin Firing Independently of Origin Density. To test whether origin density is correlated with replication timing, we defined 2 classes of origins based on origin density. Isolated origins were defined stringently as those at the center of a 200-kb window, totally included inside ENCODE regions, lacking any other origin (21 origins). Highly dense origins were defined as those having at least 2 origins within 10 kb upstream or downstream from the origin segment's edges (i.e., 3 origins in a 20-kb window). There were 10 such regions. We analyzed replication timing by cell sorting into 4 S phase fractions from early to late (S1-S4) of BrdU pulse-labeled cells. Based on the relative enrichment of nascent DNA in each of the S1-S4 fractions, we defined 5 groups of replication profiles (Fig. 3A).

In this way, we analyzed the timing of the 10 highly dense origins and found 2 early, 3 mid-early, 4 middle, and 1 mid-late replicating clusters (Fig. 3B). Thus, dense clusters of origins do not necessarily fire at the beginning of S phase and can be replicated at any moment during S phase except in late S phase. We then tested replication timing for 4 of the 21 isolated origins: 2 were mid-early, 1 was middle, and 1 was late replicated. Finally, we explored the replication timing of the ENCODE regions lacking origins (six 500-kb regions) to test whether replication forks initiated in surrounding regions passively replicated these regions. If so, we should observe a late, mid-late, or possibly middle replicated pattern in the center of these regions because of the long stretches that must be replicated before these central zones are reached. In agreement with our origin-

and either central probe of the peak has $P(X) < 10^{-5}$ and at least 1 neighboring probe has $P(X) < 10^{-4}$ or at least 2 of the neighbors have $P(X) < 10^{-4}$. For short ssDNA microarray, the less stringent criteria were (i) maximum distance (in bp) for 2 probes to be considered as neighbors = 500; (ii) a probe is considered bound if $P(X_{\text{bar}}) < 10^{-3}$ and either central probe of the peak has $P(X) < 10^{-3}$ and at least 1 neighboring probe has $P(X) < 10^{-1}$ or at least 1 of the neighbors have $P(X) < 5 \cdot 10^{-3}$.

Bioinformatics Analysis. Origin location data were loaded into a MySQL database with the data found and downloaded from the University of California at Santa Cruz ENCODE Website (<http://genome.ucsc.edu/ENCODE/encode.hg17.html>). We generated a bootstrap sample to calculate statistical significance for contingencies results between origin positions and ENCODE features. For each of the 283 origin segments, we randomly drew a segment of identical size from the same ENCODE region. We repeated this procedure 100 times to produce a set of 28,300 random segments. Then we performed a goodness of fit χ^2 test with theoretical expectation under a null hypothesis (i.e., the random position of origin) calculated from the bootstrap sample. All these χ^2 tests have 1 degree of freedom.

- Dominguez-Sola D, et al. (2007) Non-transcriptional control of DNA replication by c-Myc. *Nature* 448(7152):445–451.
- Lengronne A, Schwob E (2002) The yeast CDK inhibitor Sic1 prevents genomic instability by promoting replication origin licensing in late G(1). *Mol Cell* 9(5):1067–1078.
- Aladjem MI (2007) Replication in context: Dynamic regulation of DNA replication patterns in metazoans. *Nat Rev Genet* 8(8):588–600.
- ENCODE pc (2004) The ENCODE (Encyclopedia Of DNA Elements) Project. *Science* 306(5696):636–640.
- Birney E, et al. (2007) Identification and analysis of functional elements in 1% of the human genome by the ENCODE pilot project. *Nature* 447(7146):799–816.
- Bell SP, Stillman B (1992) ATP-dependent recognition of eukaryotic origins of DNA replication by a multiprotein complex. *Nature* 357(6374):128–134.
- Vashee S, et al. (2003) Sequence-independent DNA binding and replication initiation by the human origin recognition complex. *Genes Dev* 17(15):1894–1908.
- Danis E, et al. (2004) Specification of a DNA replication origin by a transcription complex. *Nat Cell Biol* 6(8):721–730.
- Kohzaki H, Murakami Y (2005) Transcription factors and DNA replication origin selection. *Bioessays* 27(11):1107–1116.
- Aggarwal BD, Calvi BR (2004) Chromatin regulates origin activity in Drosophila follicle cells. *Nature* 430(6997):372–376.
- Calvi BR, Byrnes BA, Kolpakos AJ (2007) Conservation of epigenetic regulation, ORC binding and developmental timing of DNA replication origins in the genus Drosophila. *Genetics* 177(3):1291–1301.
- Gilbert DM (2004) In search of the holy replicator. *Nat Rev Mol Cell Biol* 5(10):848–855.
- Gerbi SA, Bielinsky AK (1997) Replication initiation point mapping. *Methods* 13(3):271–280.
- Mesner LD, Crawford EL, Hamlin JL (2006) Isolating apparently pure libraries of replication origins from complex genomes. *Mol Cell* 21(5):719–726.
- Liu CL, Schreiber SL, Bernstein BE (2003) Development and validation of a T7 based linear amplification for genomic DNA. *BMC Genomics* 4(1):19–30.
- Cohen SM, Brylawski BP, Cordeiro-Stone M, Kaufman DG (2003) Same origins of DNA replication function on the active and inactive human X chromosomes. *J Cell Biochem* 88(5):923–931.
- Touchon M, et al. (2005) Replication-associated strand asymmetries in mammalian genomes: Toward detection of replication origins. *Proc Natl Acad Sci USA* 102(28):9836–9841.
- Lucas I, et al. (2007) High-throughput mapping of origins of replication in human cells. *EMBO Rep* 8(8):770–777.
- Hand R (1978) Eucaryotic DNA: Organization of the genome for replication. *Cell* 15(2):317–325.
- Lander ES, et al. (2001) Initial sequencing and analysis of the human genome. *Nature* 409(6822):860–921.
- Mouchiroud D, et al. (1991) The distribution of genes in the human genome. *Gene* 100:181–187.
- Delgado S, Gomez M, Bird A, Antequera F (1998) Initiation of DNA replication at CpG islands in mammalian chromosomes. *EMBO J* 17(8):2426–2435.
- Ladenburger EM, Keller C, Knippers R (2002) Identification of a binding region for human origin recognition complex proteins 1 and 2 that coincides with an origin of DNA replication. *Mol Cell Biol* 22(4):1036–1048.
- Margulies EH, et al. (2007) Analyses of deep mammalian sequence alignments and constraint predictions for 1% of the human genome. *Genome Res* 17(6):760–774.
- Koch CM, et al. (2007) The landscape of histone modifications across 1% of the human genome in five human cell lines. *Genome Res* 17(6):691–707.
- Xi H, et al. (2007) Identification and characterization of cell type-specific and ubiquitous chromatin regulatory structures in the human genome. *PLoS Genet* 3(8):1377–1388.
- Bernstein BE, et al. (2005) Genomic maps and comparative analysis of histone modifications in human and mouse. *Cell* 120(2):169–181.
- Norio P, et al. (2005) Progressive activation of DNA replication initiation in large domains of the immunoglobulin heavy chain locus during B cell development. *Mol Cell* 20(4):575–587.
- MacAlpine DM, Rodriguez HK, Bell SP (2004) Coordination of replication and transcription along a Drosophila chromosome. *Genes Dev* 18(24):3094–3105.
- Gomez M, Brockdorff N (2004) Heterochromatin on the inactive X chromosome delays replication timing without affecting origin usage. *Proc Natl Acad Sci USA* 101(18):6923–6928.
- Prioleau MN, Gendron MC, Hyrien O (2003) Replication of the chicken beta-globin locus: Early-firing origins at the 5' HS4 insulator and the rho- and betaA-globin genes show opposite epigenetic modifications. *Mol Cell Biol* 23(10):3536–3549.
- Malott M, Leffak M (1999) Activity of the c-myc replicator at an ectopic chromosomal location. *Mol Cell Biol* 19(8):5685–5695.
- Paixao S, et al. (2004) Modular structure of the human lamin B2 replicator. *Mol Cell Biol* 24(7):2958–2967.
- Schreiber M, et al. (1999) Control of cell cycle progression by c-Jun is p53 dependent. *Genes Dev* 13(5):607–619.
- Ito K, et al. (1996) c-Jun stimulates origin-dependent DNA unwinding by polyomavirus large T antigen. *EMBO J* 15(20):5636–5646.
- Remus D, Beall EL, Botchan MR (2004) DNA topology, not DNA sequence, is a critical determinant for Drosophila ORC-DNA binding. *EMBO J* 23(4):897–907.
- Watanabe Y, et al. (2002) Chromosome-wide assessment of replication timing for human chromosomes 11q and 21q: Disease-related genes in timing-switch regions. *Hum Mol Genet* 11(1):13–21.
- Rhind N (2006) DNA replication timing: Random thoughts about origin firing. *Nat Cell Biol* 8(12):1313–1316.
- Blankenberg D, et al. (2007) A framework for collaborative analysis of ENCODE data: Making large-scale analyses biologist-friendly. *Genome Res* 17(6):960–964.

The Galaxy²ENCODE program (<http://main.g2.bx.psu.edu/>) was used for other simple manipulations such as intersection, subtraction, concatenation, and merging (39).

Replication Timing Analysis. Timing analyses were made as previously described (31) excepted that S phase was divided into 4 fractions ranging from early to late S phase and designated S1 to S4.

ACKNOWLEDGMENTS. We thank T. Strick and A. West for critical reading of the manuscript and David Gilbert for helpful discussions. We thank D. Goidin from Agilent Technologies and M-C. Gendron from the Jacques-Monod Institute flow-cytometry platform for technical help. We thank A. Necsulea for help in studying correlations between computationally predicted origins and our origin segments. We thank M. Gerstein for allowing us to use ENCODE data on c-JUN and c-FOS binding sites (<http://tiling.gersteinlab.org/home/datasets.html>) and (<http://genome.ucsc.edu/ENCODE/encode.hg17.html>). Research in the laboratory of M-N.P. is supported by the Agence Nationale pour le Recherche Grant ANR 05-JCJC-0110, the Association pour la Recherche sur le Cancer, and the Ligue contre le Cancer.